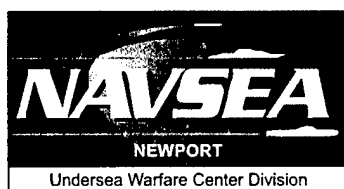


# Statistical Analysis of Detection Performance for Large Distributed Sensor Systems

Thomas A. Wettergren  
Submarine Combat Systems Directorate

20030910 099



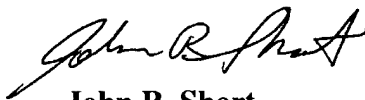
**Naval Undersea Warfare Center Division  
Newport, Rhode Island**

## **PREFACE**

This report was funded under NUWC Division Newport's Strategic Initiative Program.

The technical reviewer for this report was Roy L. Streit (Code 2002).

**Reviewed and Approved: 10 June 2003**



**John R. Short**  
**Director, Submarine Combat Systems**



# REPORT DOCUMENTATION PAGE

Form Approved  
OMB No. 0704-0188

Public reporting for this collection of information is estimated to average 1 hour per response, including the time for reviewing instructions, searching existing data sources, gathering and maintaining the data needed, and completing and reviewing the collection of information. Send comments regarding this burden estimate or any other aspect of this collection of information, including suggestions for reducing this burden, to Washington Headquarters Services, Directorate for Information Operations and Reports, 1215 Jefferson Davis Highway, Suite 1204, Arlington, VA 22202-4302, and to the Office of Management and Budget, Paperwork Reduction Project (0704-0188), Washington, DC 20503.

1. AGENCY USE ONLY (Leave blank)

2. REPORT DATE

10 June 2003

3. REPORT TYPE AND DATES COVERED

4. TITLE AND SUBTITLE

Statistical Analysis of Detection Performance for Large Distributed Sensor Systems

5. FUNDING NUMBERS

6. AUTHOR(S)

Thomas A. Wettergren

7. PERFORMING ORGANIZATION NAME(S) AND ADDRESS(ES)

Naval Undersea Warfare Center Division  
1176 Howell Street  
Newport, RI 02841-1708

8. PERFORMING ORGANIZATION  
REPORT NUMBER

TR 11,436

9. SPONSORING/MONITORING AGENCY NAME(S) AND ADDRESS(ES)

10. SPONSORING/MONITORING  
AGENCY REPORT NUMBER

11. SUPPLEMENTARY NOTES

12a. DISTRIBUTION/AVAILABILITY STATEMENT

Approved for public release; distribution is unlimited.

12b. DISTRIBUTION CODE

13. ABSTRACT (Maximum 200 words)

The problem of large-area coverage with a distributed set of short-range proximity sensors is investigated analytically. Analysis of the design tradeoffs between sensor range, sensor detection performance, and sensor false alarm performance is presented relative to the density of sensors in the field. Additionally, the impact of non-uniformity in sensor distribution on these performance assessments is quantified. The use of both individual sensor detections and coupled groups of sensor detections as a basic track-determination strategy is examined. Finally, guidance is included on strategies for making sound engineering tradeoffs based on the analytical results.

14. SUBJECT TERMS

Distributed Sensor Systems

Sensor Detection Performance

Sensor Field Distribution

Stationary and Moving Targets

Tracking Strategies

15. NUMBER OF PAGES

28

16. PRICE CODE

17. SECURITY CLASSIFICATION  
OF REPORT

Unclassified

18. SECURITY CLASSIFICATION  
OF THIS PAGE

Unclassified

19. SECURITY CLASSIFICATION  
OF ABSTRACT

Unclassified

20. LIMITATION OF ABSTRACT

SAR

## TABLE OF CONTENTS

Section	Page
LIST OF ILLUSTRATIONS .....	ii
LIST OF TABLES .....	ii
1 INTRODUCTION .....	1
2 DISTRIBUTED AREA COVERAGE MODEL .....	1
2.1 INDIVIDUAL SENSOR MODEL .....	2
2.2 FIELD DETECTION MODEL .....	3
2.2.1 Special Case 1: Uniform Distribution of Idealized Sensors .....	6
2.2.2 Special Case 2: Uniform Distribution of Non-Idealized Sensors .....	7
2.2.3 Special Case 3: Non-Uniform Distribution of Idealized Sensors .....	10
2.3 FIELD FALSE ALARM MODEL .....	13
2.3.1 Special Case 1: Non-Uniform Distribution of Sensors .....	17
2.3.2 Special Case 2: Clustering of Sensors .....	19
3 FIELD DESIGN CONSIDERATIONS .....	21
4 CONCLUSIONS .....	23

## LIST OF ILLUSTRATIONS

Figure	Page
1 Sensor Detection Geometry Showing Kinematic Constraints .....	3
2 Area $D$ for Integration Around the Target Track .....	4
3 Sensor Detection Performance for Idealized Sensor and Non-Idealized Sensor .....	7
4 Field Detection Performance as a Function of $\phi$ .....	9
5 Sample Spatial Distribution for Bivariate Gaussian with $\sigma = 50$ nmi .....	11
6 Relative Change in Field Performance for a Non-Uniform Sensor Distribution Against a Stationary Target .....	12
7 Relative Change in Field Performance for a Non-Uniform Sensor Distribution Against a Slow Moving Target .....	14
8 Relative Change in Field Performance for a Non-Uniform Sensor Distribution Against a Fast Moving Target .....	14
9 Field False Alarm Rates for Uniform and Non-Uniform Sensor Distributions .....	18
10 Detection Performance for a Field of Area 40,000 nmi <sup>2</sup> .....	22
11 False Alarm Performance for a Field of Area 40,000 nmi <sup>2</sup> .....	23

## LIST OF TABLES

Table	Page
1 Change in Field Level False Alarm Rate for Deviations from Uniformity .....	18

# **STATISTICAL ANALYSIS OF DETECTION PERFORMANCE FOR LARGE DISTRIBUTED SENSOR SYSTEMS**

## **1. INTRODUCTION**

This report develops analytical expressions for the detection performance of a sensor system composed of a large field of distributed, short-range detectors. If a field can be deployed slowly and sensors anchored to a specific location, the performance can be analyzed using traditional search theory for a large number of sensors. Furthermore, if the number of sensors is large enough so that the field coverage is very dense, visual examination of the resulting distribution of "contacts" will remove false alarms and detection performance of the field can be analyzed by examining the detection performance of an individual sensor. Neither one of these analysis techniques is appropriate if the field is sparsely populated in a random manner, and that is the type of sensor field analyzed in this report.

The analysis in this report examines the issues of detection performance of large distributed systems of proximity sensors. The effects of sensor field distribution (both uniform and non-uniform), sensor performance characteristics, and basic tracking strategy on the performance of the overall field are examined. The performance is analyzed in terms of overall probability of detection and probability of false alarm during some operation time. The report begins with a discussion of sensor performance, incorporating range dependency in ideal and non-ideal scenarios. The next section discusses field detection performance for both stationary and moving targets. The third section of the report discusses some field design strategies based on the analysis. The report concludes with a summary of the primary analysis results.

## **2. DISTRIBUTED AREA COVERAGE MODEL**

The modeling of the detection performance of a distributed sensor system requires three uncertain quantities that are modeled with random variables: individual sensor performance, sensor distribution in the field, and target location/movement. These parameters are treated as random with some known characteristics. For the purposes of this analysis, the target is fixed at constant speed and heading. The random location and orientation of the target is factored out of the problem by aligning the coordinate system of the problem so that the target track lies along the  $x$ -axis. This is performed without any loss of generality, since the sensor distributions of interest are area coverage systems. (Extensions to barrier problems will be examined in a sequel.)

## 2.1 INDIVIDUAL SENSOR MODEL

For the high signal-to-noise ratio (SNR) application of interest, each sensor is essentially an energy detector with some simple classification logic. This implies that the detection performance of an individual sensor is dependent only on the target's range to the sensor, so that the probability of a detection event for sensor  $j$  is written as  $P_{d,j} = P_d(r_j)$ , where  $P_d(r)$  is the detection probability of a characteristic sensor as a function of range  $r$ , and  $r_j$  is the target's range to the  $j^{th}$  sensor.

To examine some forms of sensor detection probability functions, several specific scenarios are considered. For a target moving at a constant speed  $v_T$  along a constant heading, the path followed by the target over a period of time  $T_{op}$  is given by a line segment of length  $L = v_T T_{op}$ . For a detection to occur, one scheme may require that the sensor lie close enough to this line segment so that the target's closest point of approach (CPA) to the sensor  $r_0$  is within the detection radius. In this scheme, a detection occurs with probability  $P_{d,j} = P_d(r_0)$ . If one further restricts the problem so that the target must stay above the detection threshold for some specified integration time  $T_{int}$ , then the CPA range for detection opportunities is limited to (see figure 1 for a geometrical sketch)

$$r_0 \leq \sqrt{R_d^2 - (v_T T_{int}/2)^2}, \quad (1)$$

where  $R_d$  is the range at which the detection threshold is exceeded. Thus, the restriction that detection opportunities occur only when the target is within range (above threshold) for the entire integration time yields

$$P_{d,j} = \begin{cases} P_d(r_j), & r_j \leq \sqrt{R_d^2 - (v_T T_{int}/2)^2} \\ 0, & \text{otherwise} \end{cases} \quad (2)$$

as the probability of a single sensor detection for a target that has CPA range  $r_j$  to the sensor  $j$ . This expression is readily evaluated given a range-based detection probability, which may be obtained from modeling or experiments. In either case, the resulting detection logic will greatly impact the individual sensor performance. For simplicity, one may wish to consider a sensor whose detection performance versus range is given by

$$P_d(r_j) = \begin{cases} P_d, & r_j \leq R_d \\ 0, & r_j > R_d \end{cases} \quad (3)$$

Of course, such an idealized sensor performance cannot be exactly obtained. To assess the performance impact of deviations from the ideal, the following model is developed:

$$P_d(r_j; \alpha) = \begin{cases} P_d, & r_j \leq R_d - \alpha/2 \\ \left(\frac{1}{2} + (R_d - r_j)/\alpha\right) P_d, & R_d - \alpha/2 < r_j < R_d + \alpha/2 \\ 0, & r_j \geq R_d + \alpha/2 \end{cases}, \quad (4)$$

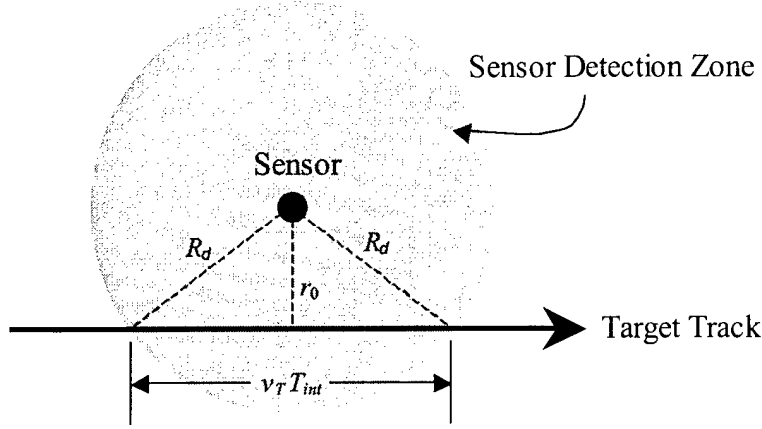


**Figure 1. Sensor Detection Geometry Showing Kinematic Constraints**

where  $\alpha > 0$  is a parameter to measure the deviation from perfect, and the limit of  $\alpha \rightarrow 0$  degenerates to the case of the ideal sensor in equation (3).

## 2.2 FIELD DETECTION MODEL

Assume that the sensors are independently and identically distributed over a nominal area according to some known spatial distribution  $p(x, y)$ . Under that assumption, the probability of a single sensor having a CPA range-to-target of less than  $r_0$  is given by

$$\Pr(r_j \leq r_0) = \iint_D p(x, y) dx dy, \quad (5)$$

where  $D$  is the region of space given by  $D = \{(x, y) : (x - x_T)^2 + (y - y_T)^2 \leq r_0^2\}$  for a target located at  $(x, y) = (x_T, y_T)$ . For the case of a stationary target, the point  $(x_T, y_T)$  remains constant throughout the time interval of operation  $T_{op}$ . In this case, the integral in equation (5) is taken as the area integral of  $p(x, y)$  over a disk of radius  $r_0$  centered about the target location. Specifically, the integral is given by

$$\begin{aligned} \Pr(r_j \leq r_0) &= \iint_D p(x, y) dx dy \\ &= \int_0^{r_0} \int_0^{2\pi} p(r \cos(\theta) + x_T, r \sin(\theta) + y_T) r d\theta dr, \end{aligned} \quad (6)$$

where the transformation to polar coordinates  $(r, \theta)$  was made to simplify the integral.

For the case of a moving target of constant heading and constant velocity, the coordinate system is re-oriented (without any loss of generality) so that the target track lies along a line of

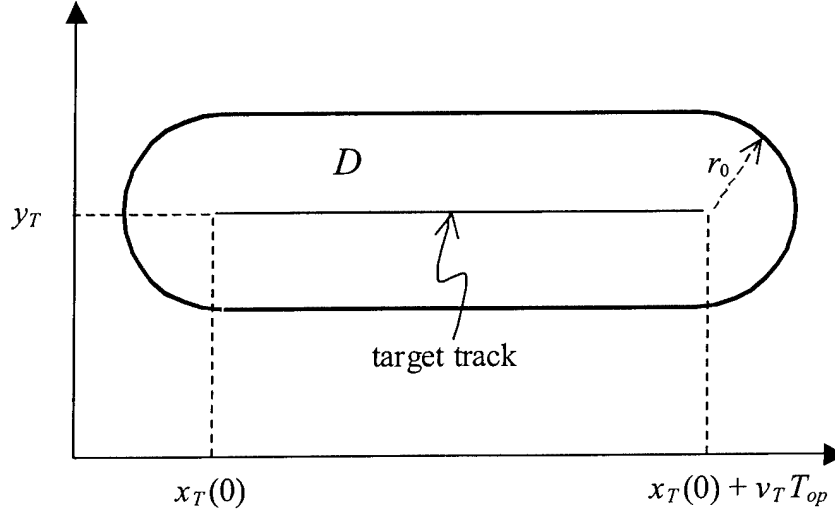


**Figure 2. Area  $D$  for Integration Around the Target Track**

constant  $y_T$ . Then the integral in equation (5) becomes

$$\begin{aligned}
 \Pr(r_j \leq r_0) &= \iint_D p(x, y) dx dy \\
 &\approx \int_{y_T - r_0}^{y_T + r_0} \int_{x_T(0)}^{x_T(0) + v_T T_{op}} p(x, y) dx dy \\
 &= \int_{-r_0}^{r_0} \int_0^{v_T T_{op}} p(x' + x_T(0), y' + y_T) dx' dy' \\
 &= \int_0^{r_0} \int_0^{v_T T_{op}} \{p(x' + x_T(0), y_T + r) + p(x' + x_T(0), y_T - r)\} dx' dr, \quad (7)
 \end{aligned}$$

where the approximation is valid for  $v_T T_{op} > r_0$ . The location of the area  $D$  in target track space is shown in figure 2. From the figure, it is clear that the approximation for large  $v_T T_{op}$  is to approximate the region around the track by a rectangle, as done in equation (7). In the case where the distance traveled by the target ( $v_T T_{op}$ ) is smaller than the detection radius  $r_0$ , a better approximation is to use the stationary target formula, which reduces the region shown in figure 2 to a circle. A more exact formula that holds for both of these cases is readily obtained by integrating the exact area of the region in figure 2; however, its evaluation is analytically intractable and therefore not included in this analysis.

Both of the formulas (see equations (6) and (7)) obtained for probability of a target coming within a certain range  $r_0$  of a sensor take the form

$$\Pr(r_j \leq r_0) = \int_0^{r_0} f(r) dr, \quad (8)$$

so that the resulting integrand  $f(r)$  in (8) is a probability density function (PDF) for the range-to-target. As a simple summary of these results, recall that these PDFs are given by the following:

#### Stationary Target Range PDF

$$f(r) = \int_0^{2\pi} p(r \cos(\theta) + x_T, r \sin(\theta) + y_T) r d\theta, \quad (9)$$

#### Moving Target Range PDF

$$f(r) = \int_0^{v_T T_{op}} \{p(x' + x_T(0), y_T + r) + p(x' + x_T(0), y_T - r)\} dx', \quad (10)$$

where the target position is given by  $(x, y) = (x_T, y_T)$ , which is either time-varying (second case) or fixed (first case).

The probability of obtaining a certain range-to-target is combined with the probability of the single sensor detection at a given range to obtain the probability of an individual sensor detecting the target. The notation  $P_{d,s}$  is used to differentiate the detection performance of an individual sensor in the field (i.e., under a distribution and with a target present) from the sensor characteristics that are described by  $P_{d,j}$  as a function of range. Since the detection performance of a given sensor is a function of range, and the range is a random variable with a known PDF, the net probability of detection for a sensor in the field is given by

$$P_{d,s} = \int_0^\infty P_{d,j} \cdot f(r) dr, \quad (11)$$

where  $T_{op}$  is the time of the operational interval over which a detection is sought, and the infinite limit will be reduced by the sensor performance (i.e., the sensor has zero detection capability beyond a certain range).

To determine the net detection performance of a field of sensors, the fact that the sensors are independently and identically distributed is used. Under that condition, the process of  $M$  sensors out of  $N$  total sensors detecting the target is viewed as a Poisson point process over the detection performance of an individual sensor. Thus, the probability of *field level detection* by  $M$  out of  $N$  sensors is given by

$$\Pr(M \text{ detect}) = \left( \frac{\phi^M}{M!} \right) e^{-\phi}, \quad \phi = N P_{d,s}. \quad (12)$$

To have *at least one detection* over the interval of time given by  $T_{op}$ , it is necessary to obtain a field level detection performance of

$$\Pr(\geq 1 \text{ detect}) = 1 - \Pr(0 \text{ detect}) = 1 - e^{-\phi}. \quad (13)$$

In a similar fashion, it is easy to show that the probability of obtaining *at least M detections* over the operation interval is given by

$$\Pr(\geq M \text{ detect}) = 1 - \sum_{m=0}^{M-1} \left( \frac{\phi^m}{m!} \right) e^{-\phi}. \quad (14)$$

### 2.2.1 Special Case 1: Uniform Distribution of Idealized Sensors

As a first special case, consider the detection performance of a uniformly distributed field of ideal sensors. In this case, the characteristics of an ideal sensor are that it has constant  $P_d$  for ranges less than some range  $R_d$  and that the  $P_d$  is zero for all ranges greater than  $R_d$ . The mathematical description of such a sensor was given in equation (3). Also, the sensor is constrained to maintain a target within range for an integration interval of  $T_{int}$  as given in equation (2). Thus, the sensor performance is given by

$$P_{d,j} = \begin{cases} P_d, & r \leq \sqrt{R_d^2 - (v_T T_{int}/2)^2} \\ 0, & r > \sqrt{R_d^2 - (v_T T_{int}/2)^2} \end{cases}. \quad (15)$$

The spatial distribution for sensor location for a uniform field over an area  $A_0$  can be written as

$$p(x, y) = \frac{1}{A_0}, \quad \forall x, y. \quad (16)$$

This greatly simplifies the range PDFs for both the stationary target and moving target. In this case, the stationary target PDF (equation (9)) becomes

$$f(r) = \int_0^{2\pi} \frac{1}{A_0} r d\theta = \frac{2\pi r}{A_0}, \quad (17)$$

and the moving target PDF (equation (10)) becomes

$$f(r) = \int_0^{v_T T_{op}} \left( \frac{1}{A_0} + \frac{1}{A_0} \right) dx' = \frac{2v_T T_{op}}{A_0}. \quad (18)$$

Combining these expressions into equation (11) for the probability of an individual sensor in the field, and recalling the identity  $\phi = NP_{d,s}$  from equation (12), the net sensor field performance as

characterized by  $\phi$  is given by

$$\begin{aligned}\phi &= \frac{2\pi N}{A_0} \int_0^{R_d} P_d \cdot r \, dr \\ &= \frac{P_d N \pi R_d^2}{A_0}\end{aligned}\tag{19}$$

for the stationary target case, and

$$\begin{aligned}\phi &= \frac{2v_T T_{op} N}{A_0} \int_0^{\sqrt{R_d^2 - (v_T T_{int}/2)^2}} P_d \, dr \\ &= \frac{P_d N (v_T T_{op}) \sqrt{4R_d^2 - (v_T T_{int})^2}}{A_0}\end{aligned}\tag{20}$$

for the moving target case. Note that the cutoff of  $R_d$  to include integration time was not performed for the stationary case since it is a kinematic-based requirement, and the use of  $v_T = 0$  in the kinematic bound yields a range of  $R_d$ .

### 2.2.2 Special Case 2: Uniform Distribution of Non-Idealized Sensors

As a second special case, consider the effects of a non-idealized sensor detection characteristic, as shown in figure 3. In this case, as described in equation (4), the performance of the sensor is degraded by tapering the sensor's effectiveness for longer ranges. The particular form of the taper is chosen so that the total area under the detection versus range curve remains constant. This constraint is a form of a power conservation law: the "total" capability of the

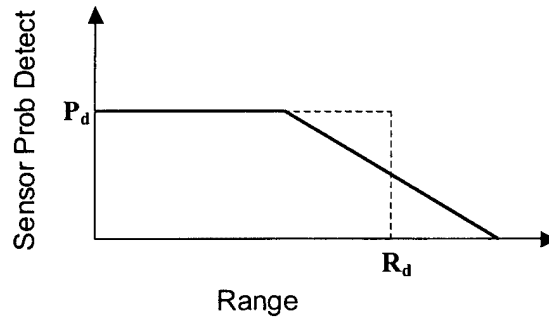


**Figure 3. Sensor Detection Performance for Idealized Sensor (Dashed Line) and Non-Idealized Sensor (Solid Line)**

sensor, in an integrated sense, is unchanged. Also, recall from equation (4) that the parameter  $\alpha$  controls the deviation from the idealized case, and  $\alpha = 0$  reduces to the idealized case.

To examine the effect of such a change in sensor performance, the analysis in the previous section is repeated for the new sensor performance curve. Since the sensor spatial distribution is uniform, the stationary and moving target PDFs are the same as in equations (17) and (18), respectively. However, the  $P_{d,j}$  term in the sensor-in-field detection performance expression (11) has changed to that given by equation (4). Applying this change to the sensor field performance characteristic  $\phi$ , one obtains

$$\begin{aligned}\phi &= \frac{2\pi N}{A_0} \left[ \int_0^{R_d-\alpha/2} P_d \cdot r \, dr + \int_{R_d-\alpha/2}^{R_d+\alpha/2} P_d \left( \frac{1}{2} + \frac{(R_d-r)}{\alpha} \right) r \, dr \right] \\ &= \frac{2\pi N}{A_0} \left[ \frac{P_d(R_d-\alpha/2)^2}{2} + P_d \left( \frac{R_d\alpha}{2} - \frac{\alpha^2}{12} \right) \right] \\ &= \frac{P_d N \pi}{A_0} \left( R_d^2 + \frac{\alpha^2}{12} \right)\end{aligned}\tag{21}$$

for the stationary case, and

$$\begin{aligned}\phi &= \frac{2v_T T_{op} N}{A_0} \left[ \int_0^{R_d-\alpha/2} P_d \, dr + \int_{R_d-\alpha/2}^{R_d+\alpha/2} P_d \left( \frac{1}{2} + \frac{(R_d-r)}{\alpha} \right) \, dr \right] \\ &= \frac{2v_T T_{op} N}{A_0} \left[ P_d \left( R_d - \frac{\alpha}{2} \right) + P_d \left( \frac{\alpha}{2} \right) \right] \\ &= \frac{2P_d N (v_T T_{op}) R_d}{A_0}\end{aligned}\tag{22}$$

for the moving target case. The kinematic requirement that the target remain in some detection radius for a given amount of time  $T_{int}$  is added to the latter expression by translating  $R_d \rightarrow \sqrt{R_d^2 - (v_T T_{int}/2)^2}$ , which creates

$$\phi = \frac{P_d N (v_T T_{op}) \sqrt{4R_d^2 - (v_T T_{int})^2}}{A_0}\tag{23}$$

for the moving target case.

The moving target case has a field-level performance characteristic  $\phi$  (see equation (23)) that is completely independent of the taper  $\alpha$ . This occurs whenever the total area under the  $P_d$  versus  $r$  curve of the sensor characteristic remains constant. Also note that the stationary target field performance characteristic as given in equation (21) is always greater than that for the ideal

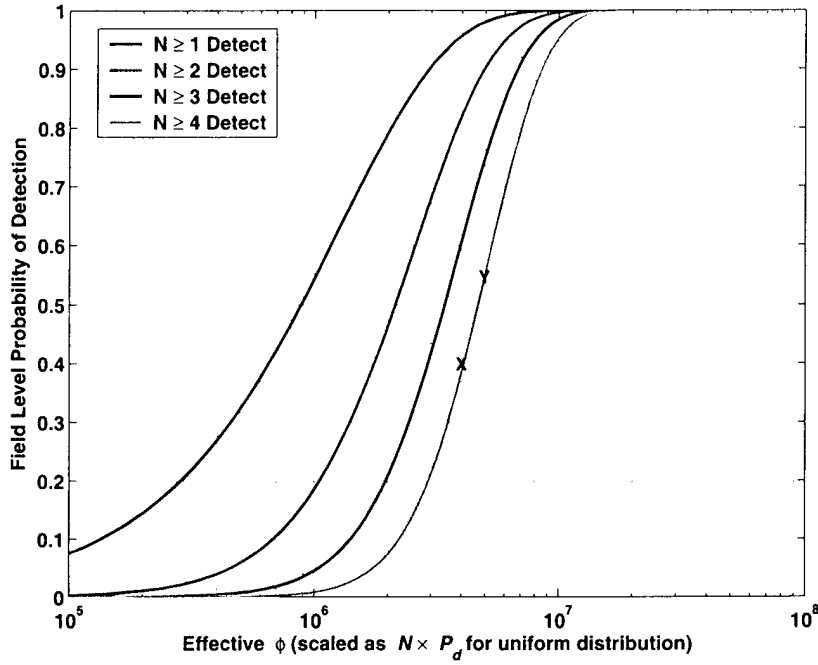


**Figure 4. Field Detection Performance as a Function of  $\phi$**

sensor ( $\alpha = 0$ ). Since greater values of  $\phi$  translate to better detection performance, a taper on the sensor detection characteristic (as long as the area is the same) will improve performance of the system, and the greater the taper, the better the system performance. Furthermore, this improvement occurs only for stationary (or very slowly moving) targets, and the performance for moving targets is unchanged.

For reference, figure 4 shows a plot of field-level performance characteristic values versus field-level probability of detection for a few detection limits (i.e., at least one detects, at least two detect, etc.). For simplicity, the horizontal axis has been normalized to be equivalent to  $\phi_0 = N \cdot P_d$  for a uniform distribution over a 100 nmi  $\times$  100 nmi area with 100 m detection radius sensors. This provides an easy reference for changes in  $\phi$ . For instance, if the nominal case has 5,000,000 sensors with a sensor  $P_d$  of 0.8, then a four-detection requirement yields a field detection 40% of the time, as shown in the figure by an X. If  $\phi$  increases by 25% over the nominal case, then the performance increases to 55% as shown by the Y on the figure.

### 2.2.3 Special Case 3: Non-Uniform Distribution of Idealized Sensors

A third special case for examination is the effect of non-uniform distributions of sensors. To simplify the analysis, the discussion is limited to bivariate Gaussian distributions of idealized sensors. This case gives some guidance on the effects of sensor clustering (due to tides, currents, etc.) that will occur over time, as well as the effect of rapid deployment, which may create a clustered distribution at the initial time. As in the previous case, the impact of the change in distribution on the field-level performance characteristic  $\phi$  is examined.

To begin the non-uniform distribution, the bivariate Gaussian distribution is formed with independent variables  $x$  and  $y$  as

$$p(x, y) = \frac{1}{2\pi\sigma^2 P_0} \exp \left[ \frac{-x^2 - y^2}{2\sigma^2} \right], \quad (24)$$

where the mean of the distribution is taken as  $(x, y) = (0, 0)$  and both variables are distributed with the same standard deviation  $\sigma$ . The choice to center the distribution at the origin is for convenience. The parameter  $P_0$  is a scaling term that represents the finite extent of the field, and it is given by

$$P_0 = \left[ \operatorname{erf} \left( \frac{L}{2\sqrt{2}\sigma} \right) \right]^2 \quad (25)$$

for a rectangular area of dimension  $L \times L$ , where  $\operatorname{erf}(\cdot)$  is the error function. An example of the relative density according to this distribution is shown in figure 5. Note that in the limit as  $\sigma \rightarrow \infty$ ,  $p(x, y) \rightarrow 1/A_0$ , which is the uniform case. (The asymptotic form of the error function for small argument is  $\operatorname{erf}(\epsilon) \approx 2\epsilon/\sqrt{\pi}$ .)

Applying the bivariate Gaussian distribution to the stationary target range PDF of equation (9), one obtains the following:

$$\begin{aligned} f(r) &= \frac{r}{2\pi\sigma^2 P_0} \int_0^{2\pi} \exp \left[ \frac{-(r \cos(\theta) + x_T)^2 - (r \sin(\theta) + y_T)^2}{2\sigma^2} \right] d\theta \\ &= \left( \frac{r}{2\pi\sigma^2 P_0} \right) \exp \left[ \frac{-r^2 - (x_T^2 + y_T^2)}{2\sigma^2} \right] \int_0^{2\pi} \exp \left[ \frac{-rx_T \cos(\theta) - ry_T \sin(\theta)}{\sigma^2} \right] d\theta \\ &\approx \left( \frac{r}{\sigma^2 P_0} \right) \exp \left( \frac{-r^2}{2\sigma^2} \right) \exp \left[ \frac{-(x_T^2 + y_T^2)}{2\sigma^2} \right], \end{aligned} \quad (26)$$

where the approximation in the third line is made by assuming the integrand in the second line to be nearly equal to one, which holds for sensor detection ranges  $r$  that are small compared to the field distribution standard deviation  $\sigma$ . Applying this value of the stationary target range PDF to the sensor field performance characteristic  $\phi$ , one obtains

$$\phi = \int_0^{R_d} P_d \cdot f(r) dr$$

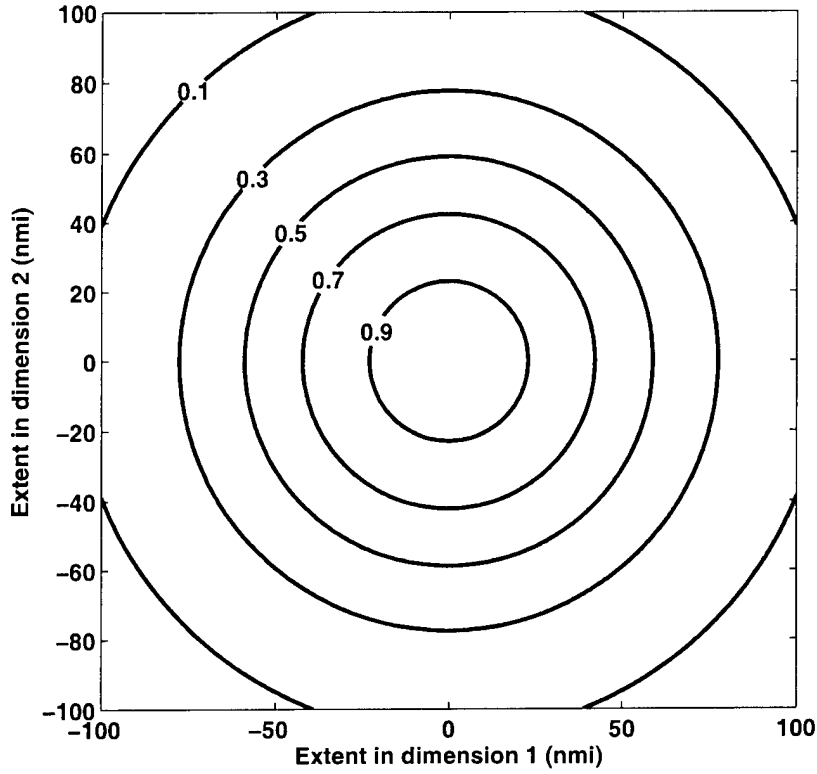


**Figure 5. Sample Spatial Distribution for Bivariate Gaussian with  $\sigma = 50$  nmi**

$$\begin{aligned}
 &= \left( \frac{P_d}{\sigma^2 P_0} \right) \exp \left[ \frac{-(x_T^2 + y_T^2)}{2\sigma^2} \right] \int_0^{R_d} r \exp \left( \frac{-r^2}{2\sigma^2} \right) dr \\
 &= \left( \frac{P_d}{P_0} \right) \exp \left[ \frac{-(x_T^2 + y_T^2)}{2\sigma^2} \right] \left[ 1 - \exp \left( \frac{-R_d^2}{2\sigma^2} \right) \right], \tag{27}
 \end{aligned}$$

where  $P_0$  is given as in equation (25).

By comparing the value of the sensor field performance characteristic  $\phi$  in equation (27) with that for the uniform field shown in (19), one can assess the impact of the non-uniformity of the field on the detection of a stationary target, which is parameterized by the distribution standard deviation  $\sigma$ . The results of this comparison are shown in figure 6 for a variety of values of  $\sigma$ . Obviously, the performance approaches the uniform as  $\sigma$  gets larger (in the limit as  $\sigma \rightarrow \infty$ , one gets the same value for equation (27) as for equation (19)). Also, the performance is better than uniform for targets near the center of the distribution (high density) and worse than uniform for those near the edges (low density). Of interest is the transition from better than uniform to worse than uniform, which seems to occur between 35 and 40 nmi from the distribution center, regardless of the distribution standard deviation  $\sigma$ .

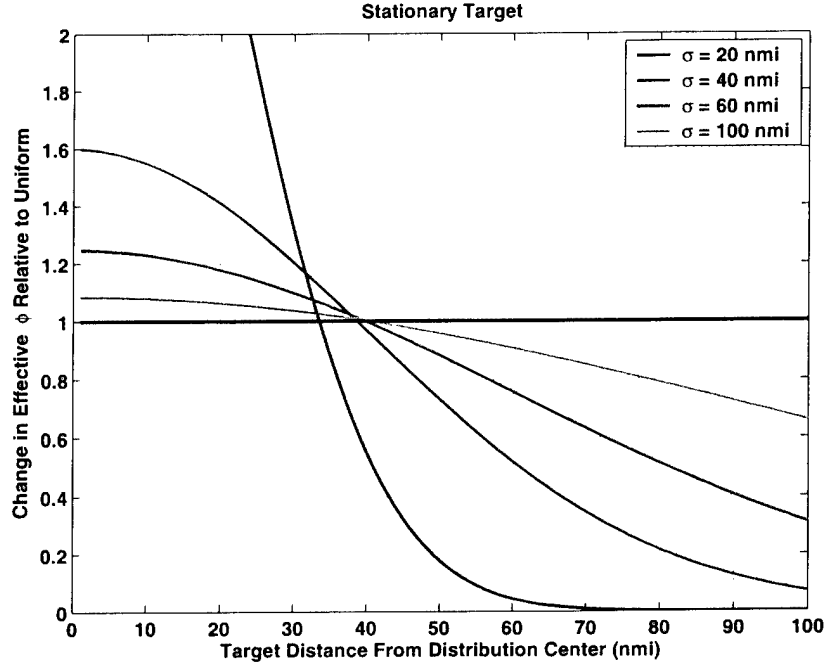


**Figure 6. Relative Change in Field Performance for a Non-Uniform Sensor Distribution Against a Stationary Target**

By performing a similar analysis of applying the bivariate Gaussian distribution to the moving target range PDF of equation (10), one obtains the following:

$$\begin{aligned}
 f(r) &= \frac{1}{2\pi\sigma^2 P_0} \int_0^{v_T T_{op}} \exp \left[ \frac{-(x' + x_T(0))^2 - (y_T + r)^2}{2\sigma^2} \right] dx' \\
 &\quad + \int_0^{v_T T_{op}} \exp \left[ \frac{-(x' + x_T(0))^2 - (y_T - r)^2}{2\sigma^2} \right] dx' \\
 &= \frac{1}{2\pi\sigma^2 P_0} \left( \exp \left[ \frac{-(y_T + r)^2}{2\sigma^2} \right] + \exp \left[ \frac{-(y_T - r)^2}{2\sigma^2} \right] \right) \\
 &\quad \times \int_0^{v_T T_{op}} \exp \left[ \frac{-(x' + x_T(0))^2}{2\sigma^2} \right] dx' \\
 &= \frac{1}{2\sqrt{2\pi}\sigma P_0} \left( \exp \left[ \frac{-(y_T + r)^2}{2\sigma^2} \right] + \exp \left[ \frac{-(y_T - r)^2}{2\sigma^2} \right] \right) \\
 &\quad \times \left[ \operatorname{erf} \left( \frac{x_T(0) + v_T T_{op}}{\sqrt{2}\sigma} \right) - \operatorname{erf} \left( \frac{x_T(0)}{\sqrt{2}\sigma} \right) \right]
 \end{aligned}$$

$$= \frac{1}{\sqrt{2\pi}\sigma P_0} \left( \exp \left[ \frac{-(y_T + r)^2}{2\sigma^2} \right] + \exp \left[ \frac{-(y_T - r)^2}{2\sigma^2} \right] \right) \operatorname{erf} \left( \frac{v_T T_{op}}{2\sqrt{2}\sigma} \right), \quad (28)$$

where the simplification in the last line is made by assuming the target path centers about  $x = 0$  (but makes no assumption about the constant  $y_T$  component of the target path). Applying this value of the moving target range PDF to the sensor field performance characteristic  $\phi$ , one obtains (using  $R = \sqrt{R_d^2 - (v_T T_{int}/2)^2}$ )

$$\begin{aligned} \phi &= \int_0^R P_d \cdot f(r) dr \\ &= \left( \frac{P_d}{\sqrt{2\pi}\sigma P_0} \right) \operatorname{erf} \left( \frac{v_T T_{op}}{2\sqrt{2}\sigma} \right) \int_0^R \left( \exp \left[ \frac{-(y_T + r)^2}{2\sigma^2} \right] + \exp \left[ \frac{-(y_T - r)^2}{2\sigma^2} \right] \right) dr \\ &= \left( \frac{P_d}{2P_0} \right) \operatorname{erf} \left( \frac{v_T T_{op}}{2\sqrt{2}\sigma} \right) \left[ \operatorname{erf} \left( \frac{y_T + R}{\sqrt{2}\sigma} \right) - \operatorname{erf} \left( \frac{y_T - R}{\sqrt{2}\sigma} \right) \right], \end{aligned} \quad (29)$$

where  $P_0$  is given as in equation (25).

By comparing the value of the sensor field performance characteristic  $\phi$  in equation (29) with that for the uniform field shown in (20), one can assess the impact of the non-uniformity of the field on the detection of a moving target, which is parameterized by the distribution standard deviation  $\sigma$ . The results of this comparison are shown in figure 7 for a variety of values of  $\sigma$ , and a target speed of 5 knots over an observation time of 12 hours. In figure 8, the result is shown for increasing the target speed to 15 knots. One observation is that the slow (5-knot) target has performance nearly identical to stationary, while the fast (15-knot) target is very different. Note that for the fast-moving target, almost all distributions show performance worse than uniform, which occurs because the target is moving fast enough to spend some of its time in the region of low sensor density. The strong dependence of the distribution on target speed is driven by the term  $v_T T_{op}$  in equation (29). Thus, a large increase in observation time  $T_{op}$  will have a similar effect on the performance as the increase in target speed. Also, the effect on increased speed may be mitigated by reducing the observation time appropriately.

### 2.3 FIELD FALSE ALARM MODEL

For the field false alarm analysis, first consider the characteristics of an individual sensor. Assume that the sensors are independent and that their statistical properties of false alarm are identically distributed. The sensor false alarm rate  $P_{fa}$  is the probability of an individual sensor classifying a detection over an integration time interval  $T_{int}$  when no target is present; that is,

$$P_{fa} = \Pr\{\text{detection during } T_{int} \mid \text{no target is present}\}. \quad (30)$$

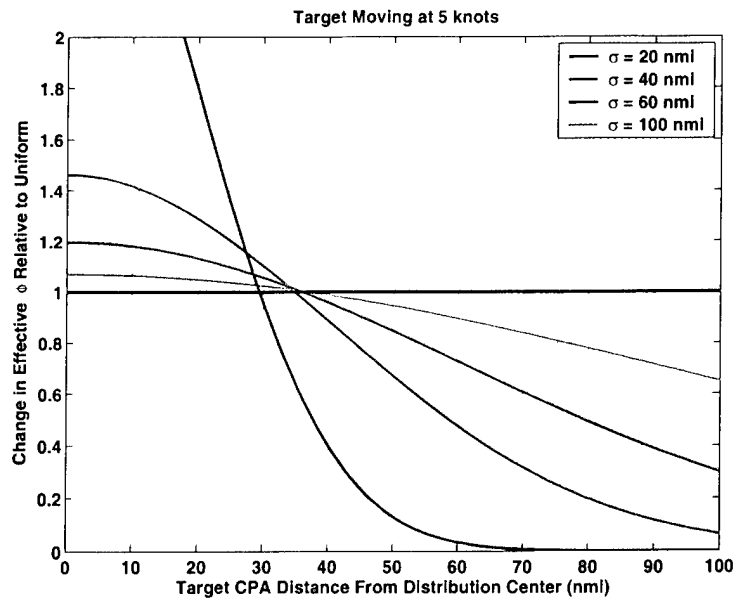


**Figure 7. Relative Change in Field Performance for a Non-Uniform Sensor Distribution Against a Slow Moving Target**

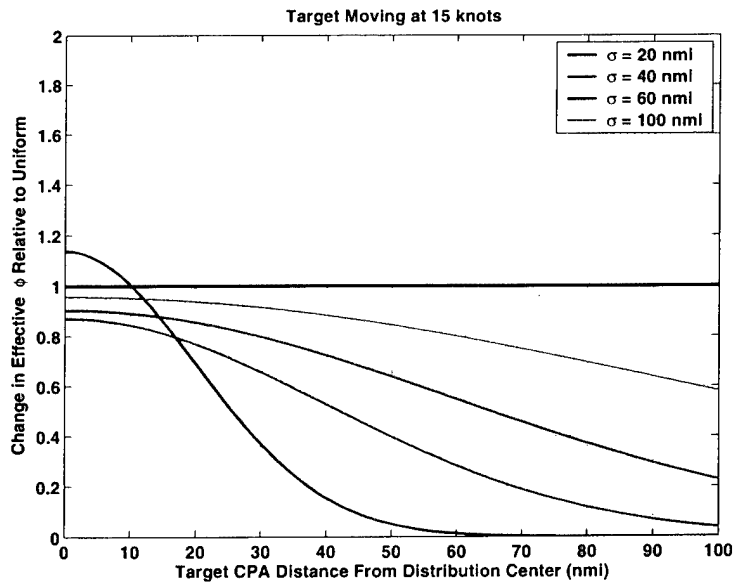


**Figure 8. Relative Change in Field Performance for a Non-Uniform Sensor Distribution Against a Fast Moving Target**

The probability of an individual sensor registering a false alarm during the time interval of operation  $T_{op}$  is given by

$$\begin{aligned} P_{fa,op} &= 1 - \Pr\{\text{no false alarm during } T_{op}\} \\ &= 1 - (1 - P_{fa})^{T_{op}/T_{int}}, \end{aligned} \quad (31)$$

where the term  $(1 - P_{fa})$  represents the probability of a false alarm not occurring during the time interval  $T_{int}$ .

The notion of a field-level false alarm is not merely to have a false alarm in the field; rather, it is to have a sequence of false alarms that mimic the behavior of a target. That is, if the detection requirement is that  $M$  out of  $N$  sensors must detect within a region of interest dictated by expected target characteristics, then the field-level false alarm requirement is that  $M$  out of  $N$  sensors must provide false alarms within a region that is consistent with expected target characteristics. At this level of analysis, one does not consider the situation where the  $M$  sensor detections are a mixture of “real” detections and false alarms. To account for the field-level false alarm requirement, one forms the probability of  $M$  false alarms occurring within a given region over the time of operation  $T_{op}$ .

Given a sensor spatial distribution of  $p(x, y)$ , the probability of a single sensor lying within the area  $D$  is

$$\Pr(\text{sensor in } D) = P_{S,D} = \iint_D p(x, y) dx dy, \quad (32)$$

where the entire region is an area of size  $A_0$ , so that

$$\iint_{A_0} p(x, y) dx dy = 1. \quad (33)$$

For uniform distributions, the probability reduces to  $P_{S,D} = A_D/A_0$ , where  $A_D$  is the area of  $D$ , which follows from  $p(x, y) = 1/A_0$  for the uniform distribution. The probability of having *exactly*  $M$  false alarms within a given region  $D$  is defined by sampling a Poisson point process within region  $D$ , with the result of (similar to equation (12))

$$\Pr(M \text{ false alarms in } D) = \left( \frac{\theta^M}{M!} \right) e^{-\theta}, \quad \theta = N_D P_{fa,op}, \quad (34)$$

where  $N_D$  is the number of sensors in region  $D$ . The value of  $N_D$  is given by

$$N_D = P_{S,D} \left( \frac{N}{P_{S,A_0}} \right) = N \cdot A_D/A_0 \quad (35)$$

for uniformly distributed fields.

The problem of interest for field-level false alarm analysis is stated as: What is the probability of *at least*  $M$  false alarms occurring within *any area* of size  $D$ ? To answer this, consider the complementary question: What is the probability that there are no areas of size  $D$  that contain at least  $M$  false alarms? The latter question is more readily assessed analytically. Thus, that probability is calculated, and the complementarity property is used to get the other probability.

The probability that there are no areas of size  $D$  that contain at least  $M$  false alarms is the same as asking for the probability that every area of size  $D$  contains less than  $M$  false alarms. Beginning with a single region of size  $D$ , from equation (34) one concludes that

$$\Pr(< M \text{ false alarms in } D) = \sum_{m=0}^{M-1} \left( \frac{\theta^m}{m!} \right) e^{-\theta}, \quad \theta = N_D P_{fa,op}. \quad (36)$$

To extend this reasoning to every region of size  $D$  containing less than  $M$  false alarms, a density argument is employed; the relative density of regions of size  $D$  over the area  $A_0$  is given by  $A_D/A_0$ , so the number of them is  $A_0/A_D$ , and since each region has an identical probability of less than  $M$  false alarms (given by equation (36)), one concludes that

$$\Pr(< M \text{ false alarms in all regions } D) = \left[ \sum_{m=0}^{M-1} \frac{(\alpha N P_{fa,op})^m}{m!} \right]^{1/\alpha} e^{-N P_{fa,op}} \quad (37)$$

for uniform distributions, where  $\alpha = A_D/A_0$ .

Now the complementarity property is used to obtain the final false alarm expression:

$$\Pr(\geq M \text{ false alarms}) = 1 - \left[ \sum_{m=0}^{M-1} \frac{(A_D N P_{fa,op}/A_0)^m}{m!} \right]^{A_0/A_D} e^{-N P_{fa,op}}, \quad (38)$$

which is the probability that there is at least one region of size  $D$  that contains at least  $M$  false alarms. The size of area  $D$  is dependent on the detection strategy employed. For the target detection situations analyzed in section 2.2, detection area  $D$  can be mapped out as the area in which a sensor has a detection opportunity, or more specifically

$$A_D = \frac{\phi A_0}{P_d N}, \quad (39)$$

where  $\phi$  depends on whether the target is stationary or moving. If searching for stationary (or slowly moving) targets, this yields

$$A_D = \pi R_d^2, \quad (40)$$

and for faster moving targets,

$$A_D = (v_T T_{op}) \sqrt{4R_d^2 - (v_T T_{int})^2}. \quad (41)$$

### 2.3.1 Special Case 1: Non-Uniform Distribution of Sensors

To consider the effects of the spatial distribution of sensors in the field, a special case is formed where the field is broken into two sections, one of high density and one of low density. For notational simplicity, assume that the region is a rectangle in the  $x$ - $y$  plane extending from  $-x_0 \leq x \leq x_0$  and  $-y_0 \leq y \leq y_0$ , for a total area of  $A_0 = 4x_0y_0$ . For the case of a uniform distribution, the results of the previous section can be applied with the use of  $A_0 = 4x_0y_0$  and  $p(x, y) = 1/A_0$  for all  $(x, y)$ .

It is now assumed that the total region is to be sectioned into two regions ( $A_1$  and  $A_2$ ) of equal size, where

$$p(x, y) = \begin{cases} p_1, & -x_0 \leq x \leq 0 & (\text{region } A_1) \\ 2/A_0 - p_1, & 0 \leq x \leq x_0 & (\text{region } A_2) \end{cases} \quad (42)$$

Since the area of each of the regions is equal to  $2x_0y_0 = A_0/2$ , one has the same total number of elements in the same total area as the uniform density case. For this special case, the probability of false alarm is formed as the probability of a false alarm occurring in either of the two regions; to simplify the model, the cases of a false alarm occurring with some sensors from each of the two regions are ignored.

The false alarm probability in region  $A_1$  is given by equation (38) with the total region area replaced with the area of  $A_1$  (which is  $A_0/2$ ) and the total number of sensors  $N$  replaced with the expected number of sensors in region  $A_1$ , which is given by

$$N_1 = \iint_{A_1} p(x, y) dx dy \left( \frac{N}{P_{S,A_0}} \right) = Np_1A_0/2. \quad (43)$$

Similarly, the number of sensors found in region  $A_2$  (which has the same area as  $A_1$ ) is given by

$$N_2 = \iint_{A_2} p(x, y) dx dy \left( \frac{N}{P_{S,A_0}} \right) = N - Np_1A_0/2, \quad (44)$$

where  $N_1 + N_2 = N$ , as expected. The probability of a false alarm occurring in either region  $A_1$  or region  $A_2$  is now given by one minus the probability that neither contains a false alarm; that is,

$$\Pr(\geq M \text{ false alarms}) = \quad (45)$$

$$1 - \left( \sum_{m=0}^{M-1} \sum_{n=0}^{M-1} \frac{(2A_D N_1 P_{fa,op}/A_0)^m (2A_D N_2 P_{fa,op}/A_0)^n}{m!n!} \right)^{A_0/(2A_D)} e^{-NP_{fa,op}}.$$

The false alarm performance of a sample area distribution relative to variations of the relative size of  $N_1$  and  $N_2$  is shown in figure 9. In this figure, the horizontal axis represents the relative

density of elements in region 1, where a relative density of 1 corresponds to the density for a uniform distribution ( $N_1 = N_2 = N/2$ ) and a relative density of 2 corresponds to all of the elements being in region 1 ( $N_1 = N, N_2 = 0$ ). The dashed lines in the figure correspond to the values of false alarm for a uniform distribution. For all three cases considered, it is apparent that small changes from uniform have negligible effect on field-level false alarm performance. Table 1 summarizes the increase in false alarm rate for a few key conditions.

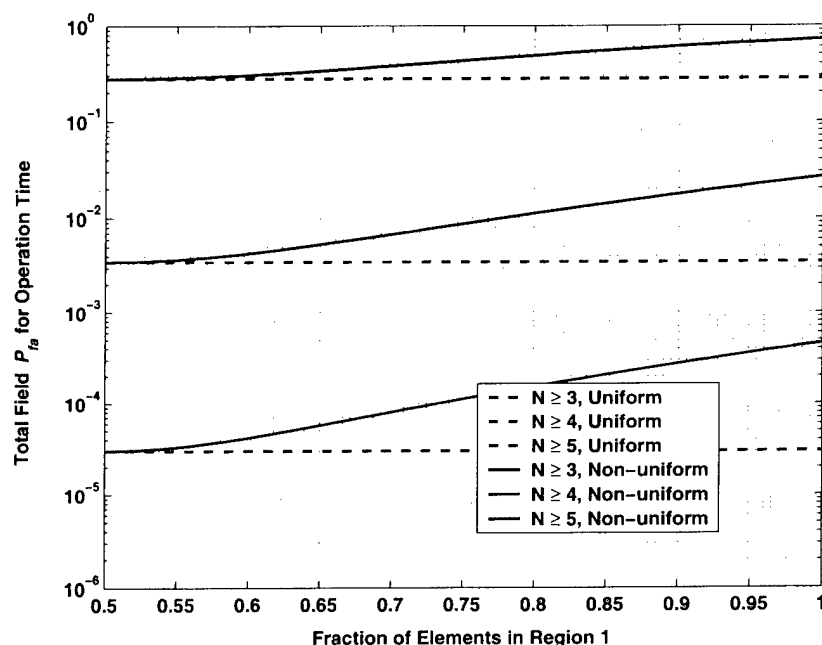


**Figure 9. Field False Alarm Rates for Uniform and Non-Uniform Sensor Distributions**

**Table 1. Change in Field Level False Alarm Rate for Deviations from Uniformity**

Case	$\rho_1 = 1.10 \times \rho_0$	$\rho_1 = 1.20 \times \rho_0$	$\rho_1 = 2.00 \times \rho_0$
$N \geq 3$	$P_{fa} = 1.02 \times P_{fa,nom}$	$P_{fa} = 1.10 \times P_{fa,nom}$	$P_{fa} = 2.58 \times P_{fa,nom}$
$N \geq 4$	$P_{fa} = 1.06 \times P_{fa,nom}$	$P_{fa} = 1.24 \times P_{fa,nom}$	$P_{fa} = 7.64 \times P_{fa,nom}$
$N \geq 5$	$P_{fa} = 1.10 \times P_{fa,nom}$	$P_{fa} = 1.40 \times P_{fa,nom}$	$P_{fa} = 15.43 \times P_{fa,nom}$

From table 1 it is clear that placing all of the elements in one half of the area produces large deviations in the false alarm rate, and the amount of that change grows with the number of required detections (i.e., the effect for  $N \geq 5$  is much larger than for  $N \geq 3$ ). It is also clear that modest changes from uniformity (on the order of 10% deviation in density) have minimal effects on the overall false alarm performance. From this analysis, it is concluded that changes in field density of 10% or less can be treated as uniform distributions for false alarm analysis.

### 2.3.2 Special Case 2: Clustering of Sensors

The analysis of fields of clustered sensors (groups of higher density in small areas) can be treated as an extension of the previous analysis of the field broken into two regions. Consider a field made of  $C$  statistically identical and independent clusters, each of which contain  $N/C$  elements. Following the method of the previous section, there are  $C + 1$  total regions:  $C$  clusters and one region of the remaining empty space. If the area of each cluster is given by  $A_C$  and there are  $N$  sensors in the total field, then the probability of false alarm for an individual cluster is given by

$$\Pr(\geq M \text{ false alarms}) = 1 - \left[ \sum_{m=0}^{M-1} \frac{(A_D(N/C)P_{fa,op}/A_C)^m}{m!} \right]^{A_C/A_D} e^{-(N/C)P_{fa,op}}. \quad (46)$$

Equation (46) is the probability of false alarm for an individual cluster.

Since the multiple clusters are assumed to be independent and identically distributed (in a statistical sense), the total field false alarm is derived from (46) by use of the complementarity property. Recall that the probability of no false alarm in a given cluster is given by one minus the probability of a false alarm. The field level false alarm probability is the probability that any cluster has a false alarm, which is given by one minus the probability that all clusters did not report a false alarm. This is given by

$$\Pr(\geq M \text{ false alarms}) = 1 - \left[ \sum_{m=0}^{M-1} \frac{(A_D N P_{fa,op} / (C A_C))^m}{m!} \right]^{C A_C / A_D} e^{-N P_{fa,op}}. \quad (47)$$

The expression for clustered-field false alarm probability (equation (47)) is the same as that for a uniform field (equation (38)) with the total area  $A_0$  replaced by the area of total cluster coverage  $C A_C$ . Note that this expression assumes the independence of clusters; that is, no consideration is given to situations where a false alarm occurs because of sensors from two neighboring clusters combining to create a potential track.

### 3. FIELD DESIGN CONSIDERATIONS

From a field design viewpoint, the objectives are low probability of false alarm and high probability of detection for a fixed total number of sensors  $N$  covering a given area  $A_0$ . Reasonable assumptions on deploying large numbers of sensors show that a uniform distribution is improbable. However, both the detection and false alarm analyses show that only moderate deviations from uniformity are acceptable before performance degrades. For the examples considered, one desires spatial standard deviations on the order of tens of nautical miles (see figure 8) for detection performance and density deviations of no more than 20% (see figure 9) to minimize impact on false alarm. This leads to the conclusion that a practical design solution is to deploy a field of clusters of sensors. Each cluster can be held to a reasonably uniform distribution by making the clusters small enough and spacing them within the field to maximize detection performance over the entire area.

Some ideas for cluster distributions include widely-separated high-density rows of sensors, checkerboard distributions of high-density "squares" of sensors, and random distributions of clusters of varying sizes. For the analysis in this report, consider the nominal problem of searching a 40,000-nmi<sup>2</sup> area for a contact of speed up to 5 knots. The probability of detection for the clustered field is the net probability of detection for each of the clusters; that is,

$$P_{d,field}(T_C) = 1 - (1 - P_{d,cluster})^C, \quad (48)$$

where  $C$  is the number of clusters. The probability of detection within a cluster ( $P_{d,cluster}$ ) is given by equation (14), where  $N$  is replaced by  $N/C$  and  $\phi$  is computed over the area of a cluster. This expression can be modified by the changes shown in sections 2.2.1-2.2.3 for modifications to the ideal sensors in a uniform distribution within a cluster. This probability is only for the interval of time it takes the target to transit a nominal cluster ( $T_C = 2\sqrt{A_C/\pi}/v_T$ ). Since there are many such opportunities within the entire field, the total probability of detection is given by

$$\begin{aligned} P_{d,field}(T_{op}) &= 1 - (1 - P_{d,field}(T_C))^{T_{op}/T_C} \\ &= 1 - (1 - P_{d,cluster})^{C \cdot T_{op}/T_C}. \end{aligned} \quad (49)$$

The probability of field-level false alarm for the clustered field is given by equation (47), which will hold as long as the sensor density within a cluster doesn't vary by more than 10%.

To show how these expressions are used to assist with field design, they are evaluated for a specific scenario. The field size and target speed are as given in the previous paragraph. The sensors are all ideal with a  $P_d = 0.9$  out to a range of  $R_d = 100$  m. The integration time is assumed to be 40 seconds and the total operation time under which a target is searched for is 8 hours. Each sensor has a false alarm rate of  $10^{-5}$  over the integration interval. The field is populated with  $N = 500,000$  such sensors. Simple calculation shows the total detection area

coverage to be  $N\pi R_d^2 = 3,927 \text{ nmi}^2$ , which is only 10% of the total search area, thus creating a sparse sensor field.

For this sparse sensor field, it is necessary to require multiple sensor detection reports before classifying a detection as accurate. Consider the effects of taking  $N \geq 3$ ,  $N \geq 4$ , and  $N \geq 5$  sensor detection reports within a prospective target track. By evaluating the field-level detection and false alarm statistics, the utility of varying degrees of clustering is determined. The probability of detection for the field at various levels of clustering (no cluster,  $C = 100$ ,  $C = 1000$ ,  $C = 10,000$ ) is shown in figure 10 as a function of cluster size. It is obvious that detection performance is always less for clustering than for the uniform field. Also note that each value of  $C$  (number of clusters) has a corresponding “sweet spot” in cluster size. As long as the cluster is sized according to this sweet spot, detection performance is nearly identical for the various cluster sizes. However, the width of the sweet spot (how tightly held cluster size needs to be) decreases with larger numbers of clusters. This makes the most practical solution to have a relatively smaller number of clusters and keep the cluster size in the sweet spot.

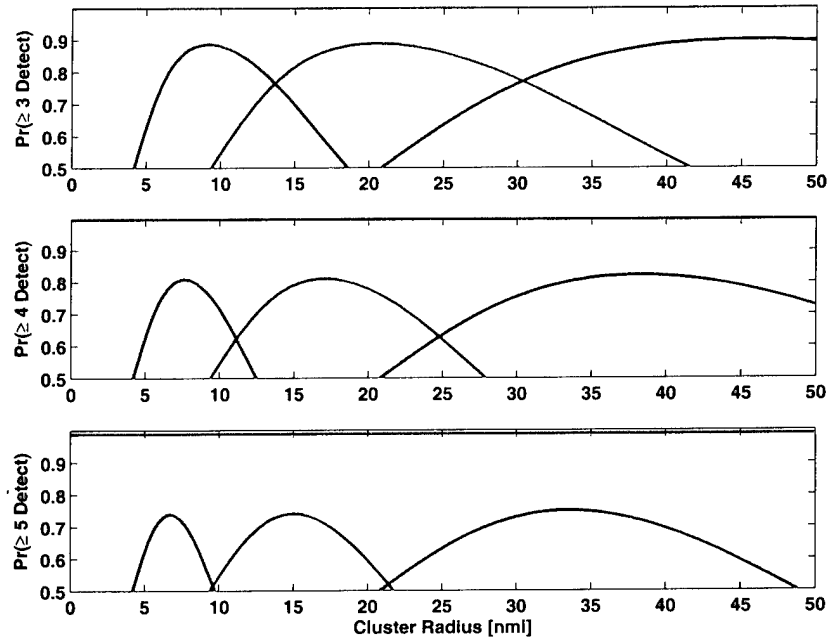


**Figure 10. Detection Performance for a Field of Area 40,000 nmi<sup>2</sup>**  
(Pink: Uniform Distribution, Blue:  $C=20$ , Green:  $C=100$ , Red:  $C=500$ )

The motivation for clustering was to decrease the false alarm rate for the field. The effects of clustering on field false alarm rate are shown in figure 11 for the same levels of clustering (no cluster,  $C = 100$ ,  $C = 1000$ ,  $C = 10,000$ ). Here it is obvious that clustering improves the false alarm performance (compared to uniform) if the clusters are made large enough. Furthermore, the

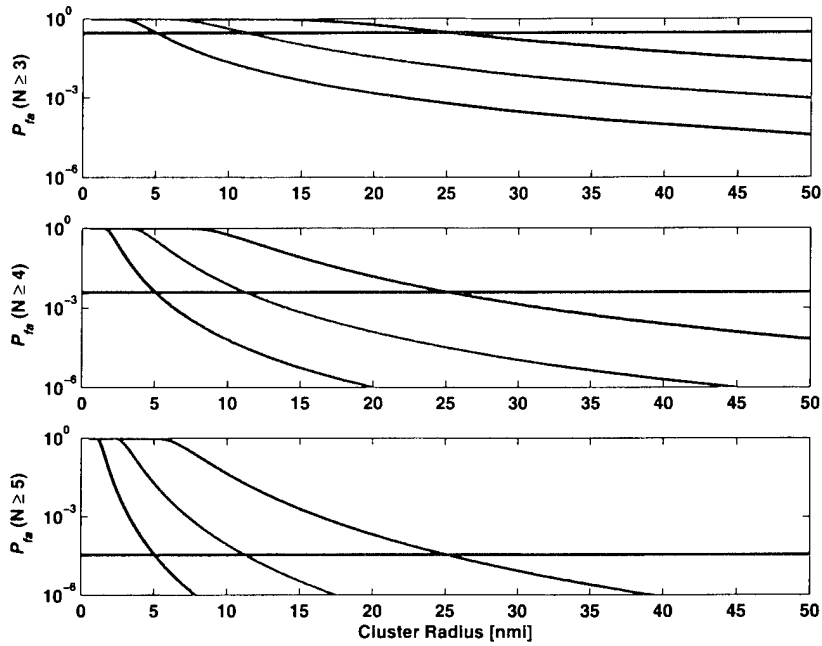


**Figure 11. False Alarm Performance for a Field of Area 40,000 nmi<sup>2</sup>**  
(Pink: Uniform Distribution, Blue: C=20, Green: C=100, Red: C=500)

cluster size must be larger for smaller numbers of clusters. Thus, a practical guideline may be derived that the cluster size be chosen as the largest cluster where the density can be held relatively constant (within 10% variation). Using this guideline, the number of clusters is chosen so that cluster size lands in the “sweet spot” for detection performance. In this way, a reasonably optimal tradeoff is made between false alarm performance and detection performance. Obviously, these decisions must be made with regard to meeting any set absolute performance criteria (i.e.,  $P_d$  must be greater than  $X$ , and  $P_{fa}$  must be less than  $Y$ ); however, this analysis shows some of the tradeoffs that can be advantageously made.

#### 4. CONCLUSIONS

This report has provided an analytical derivation of the important tradeoffs involved in the performance of large distributed systems of proximity sensors. Throughout the analysis, realistic features were added to examine their impact on modifying the idealized system’s resulting performance. A summary of the important results follows:

- Sensor detection performance versus range is driven by the total area under a  $P_d$  versus range curve.
- Field detection performance for moving targets is generally better than for stationary targets, especially when an  $M$  out of  $N$  detection criterion is applied to determine prospective targets.
- Field probability of detection is lowered by increasing the number of required detections; however, probability of false alarm is lowered by a greater amount.
- Non-uniformity of the spatial distribution degrades field detection performance in general. The degradation is larger for faster moving targets than for slow-moving or stationary targets. Also, the degradation is not very severe if the standard deviation of the distribution is on the order of the field size.
- Non-uniformity of the spatial distribution degrades field false alarm performance in general. The degradation is moderate if the field sensor density does not vary by more than 10%. The degradation with non-uniformity is worse for larger numbers of required detections.
- Clustering of sensors provides an effective way to lower field probability of false alarm at the expense of reduced field probability of detection. However, the effect on detection can be minimized by choosing the cluster size and number of clusters carefully to lie in a detection “sweet spot.”
- Clustering of sensors provides a means of mitigating the effects of non-uniformity, since the degree of non-uniformity is important only within a cluster. Thus, since clusters are geometrically small, their distributions are easier to control within acceptable bounds.

These guidelines and the supporting calculations show that it is possible to optimize the performance of a sensor field for a given sensor type by choosing a proper clustering scheme, distribution requirement, and number of detections to generate a track. It is intended that the analysis contained in this report be used and expanded to assist in the design of optimally performing systems of large numbers of distributed sensors. Extensions that should be done include combined analysis with tracking systems, analysis of the effects of mixed (real plus false alarm) reports, analysis of fields of mixed sensor type, and numerical optimization of field performance in a Pareto optimal sense.

## INITIAL DISTRIBUTION LIST

Addressee	No. of Copies
Office of Naval Research (ONR 321 – O. Allen; ONR 321SS – J. McEachern, C. Traweek)	3
Advanced Research Projects Agency (CAPT D. Babcock, G. Roesler)	2
Sandia National Laboratories (J. Feddema)	1
Defense Technical Information Center	2